Med Chem Res
DOI 10.1007/s00044-016-1659-y

MEDICINAL CHEMISTRY RESEARCH

ORIGINAL RESEARCH

Permeability of novel 4′-*N*-substituted (aminomethyl) benzoate-7-substituted nicotinic acid ester derivatives of scutellarein in Caco-2 cells and in an in vitro model of the blood-brain barrier

Yu Ou[1] · Min Luo[2] · Yong-Xi Dong[2] · Hang Su[2] · Xiao-Zhong Fu[2] · Yu-Feng Cha[2] · Shun Zhang[2] · Yong-Long Zhao[2] · Yong-Jun Li[3] · Yong-Lin Wang[3]

Received: 24 July 2015 / Accepted: 4 July 2016

Abstract A series of 4′-*N*-substituted (aminomethyl) benzoate-7-substituted nicotinic acid ester derivatives of scutellarein was designed and synthesized. Evaluation of physiochemical properties showed that the newly designed compounds had greater chemical stability and aqueous solubility than scutellarin or scutellarein. The permeabilities ($P_{app\ AP\ to\ BL}$) of compounds **7b** and **7e** in Caco-2 cells were 5.9-fold and 3.7-fold higher than that of scutellarin, and 3.7-fold and 2.4-fold higher than that of scutellarein. The permeabilities ($P_{app\ AP\ to\ BL}$) of compounds **7b** and **7e** in an in vitro model of the blood–brain barrier were 9.7-fold and 5.9-fold higher than that of scutellarin, and 9.2-fold and 5.6-fold higher than that of scutellarein.

Keywords Scutellarein · Nicotinic acid · Caco-2 cell · Permeability · In vitro blood–brain barrier model

Electronic supplementary material The online version of this article (doi:10.1007/s00044-016-1659-y) contains supplementary material, which is available to authorized users.

Yu Ou and Min Luo contributed equally to this work

✉ Xiao-Zhong Fu
xiaozhong_fu@sohu.com

[1] Pharmacy Department, Guiyang Women and Children's Hospital and Health Institute, Guiyang 550001 Guizhou, China

[2] Engineering Research Center for the Development and Application of Ethnic Medicine and TCM (Ministry of Education), School of Pharmacy, Guizhou Medical University, Guiyang 550004 Guizhou, China

[3] Guizhou Provincial Key Laboratory of Pharmaceutics, Guizhou Medical University, Guiyang 550004 Guizhou, China

Introduction

Scutellarin (4′, 5, 6-trihydroxyflavone-7-glucuronide) is the main active ingredient in the Chinese herb *Erigeron breviscapus* (Vant.) Hand.-Mazz (Zhang et al., 2000), which has been used in China since 1984 to treat acute cerebral infarction as well as paralysis induced by cerebrovascular diseases such as hypertension, cerebral thrombosis, and cerebral hemorrhage (Pan et al., 2008; Zhou et al., 2006). Scutellarin significantly attenuates the cytotoxicity of H_2O_2 and reduces the intracellular accumulation of reactive oxygen species (ROS), cellular mechanisms that may account for its neuroprotective effects (Hong and Liu, 2000).

Large amounts of the aglycone scutellarein have recently been identified in urine and plasma samples following oral administration of scutellarin to subjects in clinical trials. This indicates that scutellarin is hydrolyzed in the colon to scutellarein, which is then absorbed. Pharmacokinetic and pharmacodynamic studies have shown that scutellarein has higher relative bioavailability (301.8 %) and ROS-scavenging activity than scutellarin (Che et al., 2007; Chen et al., 2006), suggesting that scutellarein might be the true bioactive component of *E. breviscapus* (Zhang et al., 2003; Ju et al., 2005).

Although scutellarein has more potent antioxidant activity and a higher absorption rate than scutellarin, its clinical use is hindered by several factors. Structurally, scutellarein contains four hydrophilic phenolic groups and a hydrophobic 2-phenyl-4H-chromen-4-one core. These structural features result in very poor absorption, distribution, metabolism, and excretion (ADME) properties, including very low absolute bioavailability (7 %) in beagle dogs (Ge et al., 2003) and low blood-brain barrier (BBB) permeability (Hu et al., 2005). These shortcomings have been attributed to its very low solubility in both water (14 μg/mL) and lipid (log $P = 0.96$) (Dai et al., 2015) as

Published online: 26 July 2016

well as intestinal instability and rapid hepatic first-pass elimination (Wang et al., 2011).

A number of prodrug strategies, including scutellarein carbamates, scutellarein-*O*-alkylamines and scutellarein L-amino acid esters, have been used successfully to improve the ADME properties of scutellarein (Sang et al., 2015; Sang et al., 2015; Fu et al., 2011). The phenolic hydroxyl groups of scutellarein provide important 'synthetic handles' for the structural modification of scutellarein and facilitate the design and synthesis of novel prodrugs with the potential for improved bioactivity and physiochemical properties.

A number of strategies have been proposed (Hansch et al., 1987; Young et al., 1988; Bradbury, 1984) to improve BBB penetration. These involve modification of the parent structure to give prodrugs that are substrates for endogenous BBB transporters, such as those for carboxylic acids, amino acids, hexose derivatives, and small molecular weight peptides (Zhang et al., 2011; Bonina et al., 2000; Malakoutikhah et al., 2008).

Nicotinic acid esters, such as 10-*O*-nicotinate ginkgolide B (Wu et al., 2012), 3-*O*-nicotinate penicillin V (Bartzatt, 2005), and nicotinic acid-mustard conjugate (Rajesh, 2014), particularly, are transported across the BBB with high efficiency. The efficient transport of nicotinic acid esters across the BBB have been attributed to their ability to act as substrates for the monocarboxylate transporter 1 (MCT1), a proton-linked membrane transport protein that is expressed on both luminal and abluminal membranes of brain capillary endothelial cells (Enerson and Drewes, 2003). In a previous study, we designed and synthesized a series of 4′-*N*-substituted (aminomethyl) benzoate derivatives of scutellarein that showed improved physiochemical properties and enhanced in vitro antioxidant activity (Fu et al., 2011). In our present search for scutellarein derivatives with high BBB permeability, Caco-2 cell permeability and antioxidant activity, we have adopted the substructure combination principle to design compounds in which substituted nicotinic acid esters are attached to the 7-position of 4′-*N*-substituted (aminomethyl) benzoate derivatives of scutellarein.

We have prepared six novel 4′-*N*-substituted (aminomethyl) benzoate-7-substituted nicotinic acid ester derivatives of scutellarein (**7a**–**7f**) and evaluated their physiochemical properties, Caco-2 cell permeability, and permeability in an in vitro model of the BBB. Our results should afford valuable information for the design of new scutellarin prodrugs.

Experimental section

Materials and methods

Scutellarin (purity > 95 % by high performance liquid chromatography [HPLC]) was provided by Feng shang jian Pharmaceutical Co., Ltd. (Yunnan, China). Scutellarein (**2**), 6,7-ketal protected scutellarein (**3**), 4′-*N*-substituted (aminomethyl) benzoic acids (**4a**–**4d**), and 4′-*N*-substituted (aminomethyl) benzoate derivatives of scutellarein (**5a**–**5d**) were synthesized as previously described (Fu et al., 2011; Chen et al., 2005). Other chemicals were 97–99 % pure and were purchased from Sinopharm Chemical Reagent Co., Ltd. ^{1}H-NMR spectra (reference tetramethylsilane for δ_H, *J* values in Hz) were recorded using a Varian Mercury 400 spectrometer. Low-resolution mass spectra were obtained using an ACQUITY TQD low-resolution mass spectrometer (Waters, USA), and high-resolution mass spectra were obtained using a microTOFQ II ESI-Q-ToF LC/MS/MS instrument (Bruker Daltonics). Flash chromatography was carried out on silica gel (200–300 mesh) and chromatographic solvent proportions are expressed on a volume:volume basis. Caco-2 cells were obtained from the Shanghai Institute of Material Medica. Permeabilities in Caco-2 cells and in the in vitro BBB model were evaluated using an ACQUITY UPLC instrument (Waters, USA). Samples were separated using a BEH C 18 column (2.1 mm × 50 mm, 1.7 µm), equipped with a BEH C18 VanGuard pre-column (2.1 mm × 5 mm, 1.7 µm). All anhydrous solvents were distilled from CaH_2 or Na/benzophenone prior to use.

*Preparation of 4′-N-substituted (aminomethyl) benzoate-7-substituted nicotinic acid ester derivatives of scutellarein (**7a**–**7f**)*

The synthetic route is outlined in Scheme 1

A 100 mL, three-necked, round-bottomed flask, fitted with a nitrogen inlet adapter, was charged with 6-chloronicotinic acid (500.0 mg, 3.18 mmol) and substituted amine (15.92 mmol). The resulting mixture was stirred for 30 min until it became homogeneous and then stirred at 120–130 °C for 6 h, when thin layer chromatography (TLC) (eluent:dichloromethane/methanol/acetic acid (15:1:1, v/v/v)) indicated that the reaction was complete. The resulting mixture was partially purified by flash column chromatography on silica gel, using dichloromethane/methanol/acetic acid (30:1:1, v/v/v) as the eluent. The resulting crude product was dissolved in ethanol (10 mL) and precipitated by the addition of acetic acid (0.5 mL). This process was repeated three times and the suspension was then centrifuged for 10 min at 4000 g. The sediment was collected and washed with Et_2O to obtain pure 6-substituted nicotinic acid (**6a**–**6c**).

A 50 mL, three-necked, round-bottomed flask, fitted with a nitrogen inlet adapter, was charged with 4′-*N*-substituted (aminomethyl) benzoate derivative of scutellarein (**5a**–**d**) (0.21 mmol), 6-substituted nicotinic acid (**6a**–**c**) (0.27 mmol), 4-dimethylaminopyridine (0.21 mmol), CH_2Cl_2 (25

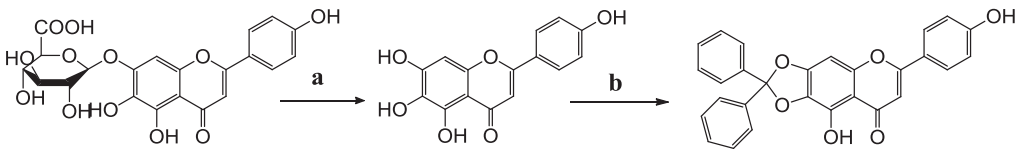

1 2 3

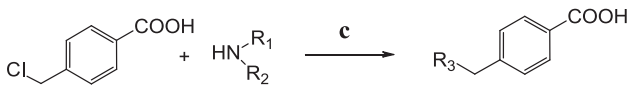

4a-d

R_3 =

4a 4b 4c 4d

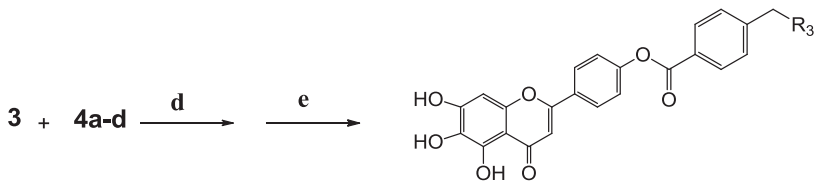

5a-d

R_3 =

5a 5b 5c 5d

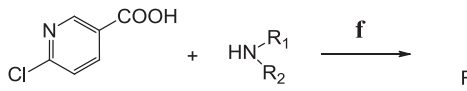

6a-c

R_4 =

6a 6b 6c

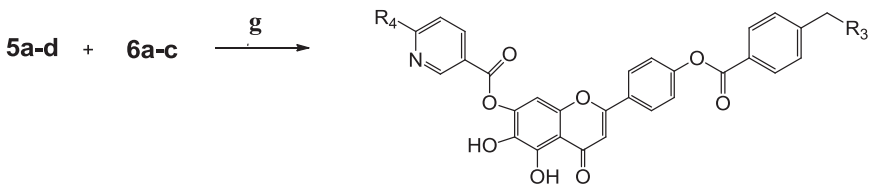

7a-f

7a: R_3 = R_4 =

7b: R_3 = R_4 =

7c: R_3 = R_4 =

7d: R_3 = R_4 =

7e: R_3 = R_4 =

7f: R_3 = R_4 =

◀ **Scheme 1** Reagents and conditions: **a** 8 % dilute sulfuric acid aqueous, 90 °C, 20 h; **b** diphenyldichloromethane, DMAP, DEME, 170 °C; **c** anhydrous EtOH, reflux 24 h; **d** DMAP, DCC, anhydrous THF, rt, 12 h; **e** CH_3COCl/MeOH, EtOAc, −5–0 °C, 10 h; **f** N_2 atmosphere, 120–130 °C, 12 h; **g** DMAP, DCC, CH_2Cl_2, rt, 20 h

mL), and dimethyl sulphoxide (DMSO) (1 mL). The resulting mixture was stirred for 30 min until it become homogeneous and a solution of dicyclohexylcarbodiimide (0.21 mmol) in CH_2Cl_2 (5.0 mL) was then added slowly to the solution. After stirring at room temperature for 24 h, the mixture was filtered and concentrated in vacuo. The residue was purified by flash column chromatography on silica gel using gradient elution with chloroform/methanol (100:1 to 30:1, v/v) to give the target compound. Products **7a**–**f** were obtained in this way as yellow solids in 36.4–45.1 % yield.

*5,6-dihydroxy-4-oxo-2-(4-((4-(pyrrolidin-1-ylmethyl) benzoyl)oxy)phenyl)-4H-chromen-7-yl 6-(piperidin-1-yl) nicotinate (**7a**)*

Yellow solid, yield: 36.4 %, m.p. 242–244 °C.^{1}H NMR (400 MHz, DMSO-d_6): $\delta = 12.95$ (brs, 1H, 5-OH), 8.74(s, 1H, pyr–H_2), 8.18(d, $J = 8.0$ Hz, 2H, Ar″–$H_{2,6}$), 8.08 (d, $J = 8.0$ Hz, 2H, Ar′–$H_{2,6}$), 8.02 (dd, $J_1 = 8.0$ Hz, $J_2 = 2.4$ Hz, 1H, pyr–H_4), 7.50–7.46 (m, 2H, Ar″–$H_{3,5}$), 7.28–7.20 (m, 2H, Ar′–$H_{3,5}$), 7.03 (s, 1H, Ar–H_3), 6.69 (s, 1H, Ar–H_8), 6.52(d, $J = 8.0$ Hz, 1H, pyr–H_5), 3.55–3.44 (m, 6H, 3 × CH_2N), 2.46–2.41(m, 4H, 2 × CH_2N), 1.99–1.93 (m, 10H, 5 × CH_2). ^{13}C NMR (100 MHz, DMSO-d_6) $\delta = 182.7$ (C, C-4), 164.6 (C, C-7′), 163.7 (C, C-2), 163.3 (C, pyr–CO), 159.1 (C, C-6), 157.8(C, C-5), 154.5 (C, C-9), 153.9 (CH, pyr–C2), 153.0 (C, C-4′), 152.2 (C, C-7), 145.8(C, C-4″), 138.4 (CH, pyr–C4), 130.4 (2 × CH, C-2″, C-6″), 129.7 (2 × CH, C-2′, C-6′), 129.4 (2 × CH, C-3″, C-5″), 128.7 (2 × CH, C-3′, C-5′), 127.5 (C, pyr–C3), 123.3 (C, C-10), 123.1 (CH, pyr–C5), 111.7 (CH, C-3), 106.5 (CH, C-8), 63.4 (CH_2, CH_2N), 53.0 (2 × CH_2, 2 × CH_2N), 47.2 (2 × CH_2, 2 × CH_2N), 25.7 (2 × CH_2, 2 × ***C***H_2CH_2N), 25.3 (2 × CH_2, 2 × ***C***H_2CH_2N), 24.1 (CH_2, CH_2***C***H_2CH_2). ESI-MS (*m/z*): 662.3[M+H]$^+$. HRESIMS *m/z* (pos): 662.2489 $C_{38}H_{36}N_3O_8$ (calcd. 662.2497).

*5,6-dihydroxy-4-oxo-2-(4-((4-(piperidin-1-ylmethyl) benzoyl)oxy)phenyl)-4H-chromen-7-yl 6-(pyrrolidin-1-yl) nicotinate (**7b**)*

Yellow solid, yield: 45.1 %, m.p. 246–248 °C.^{1}H-NMR (400 MHz, DMSO-d_6): $\delta = 12.93$ (brs, 1H, 5-OH), 8.76 (s, 1H, pyr–H_2), 8.17 (d, $J = 8.4$ Hz, 2H, Ar″–$H_{2,6}$), 8.08 (d, $J = 8.0$ Hz, 2H, Ar′-$H_{2,6}$), 8.02 (dd, $J_1 = 8.8$ Hz, $J_2 = 2.0$ Hz, 1H, pyr–H_4), 7.51–7.46 (m, 4H, Ar″–$H_{3,5}$ and Ar′–$H_{3,5}$), 6.99 (s, 1H, Ar–H_8), 6.68 (s, 1H, Ar–H_3), 6.52 (d, $J = 8.0$ Hz, 1H, pyr–H_5), 3.54–3.45 (m, 6H, 3 × CH_2N), 2.34–2.27 (m, 4H, 2 × CH_2N), 1.50–1.47 (m, 6H, 3 × CH_2), 1.37–1.35 (m, 4H, 2 × CH_2). ^{13}C NMR (100 MHz, DMSO-d_6) $\delta =$ 182.6 (C, C-4), 164.6 (C, C-7′), 163.9 (C, C-2), 163.2 (C, pyr–CO), 159.2(C, C-6), 158.2 (C, C-5), 154.6 (C, C-9), 153.9 (CH, pyr–C2), 153.0 (C, C-4′), 152.2 (C, C-7), 138.7 (C, C-4″), 138.5 (CH, pyr–C4), 130.5 (2 × CH, C-2″, C-6′′), 129.9 (2 × CH, C-2′, C-6′), 128.9 (2 × CH, C-3″, C-5″), 128.6 (2 × CH, C-3′, C-5′), 127.7 (C, pyr–C3), 123.3 (C, C-10), 123.1 (CH, pyr–C5), 111.7 (CH, C-3), 106.4 (CH, C-8), 62.6 (CH_2, CH_2N), 54.3 (2 × CH_2, 2 × CH_2N), 47.3 (2 × CH_2, 2 × CH_2N), 26.0 (2 × CH_2, 2 × CH_2CH_2N), 25.9 (2 × CH_2, 2 × ***C***H_2CH_2N), 24.2 (CH_2, CH_2***C***H_2CH_2). ESI-MS (*m/z*): 662.3 [M+H]$^+$. HRESIMS *m/z* (pos): 662.2478 $C_{38}H_{36}N_3O_8$ (calcd. 662.2497).

*5,6-dihydroxy-4-oxo-2-(4-((4-(piperidin-1-ylmethyl) benzoyl)oxy)phenyl)-4H-chromen-7-yl 6-(piperidin-1-yl) nicotinate (**7c**)*

Yellow solid, yield: 45.4 %, m.p. 264–266 °C.^{1}H-NMR (400 MHz, DMSO-d_6): $\delta = 12.94$(brs, 1H, 5-OH), 8.74 (s, 1H, pyr–H_2), 8.17 (d, $J = 8.0$ Hz, 2H, Ar″–$H_{2,6}$), 8.08 (d, $J = 8.0$ Hz, 2H, Ar′–$H_{2,6}$), 8.01 (dd, J_1=8.0 Hz, $J_2 = 2.0$ Hz, 1H, pyr–H_4), 7.51–7.46 (m, 4H, Ar″-$H_{3,5}$ and Ar′–$H_{3,5}$), 7.00 (s, 1H, Ar–H_8), 6.88 (d, $J = 8.0$ Hz, 1H, pyr–H_5), 6.67 (s, 1H, Ar–H_3), 3.68–3.65 (m, 6H, 3 × CH_2N), 2.47–2.45 (m, 4H, 2 × CH_2N), 1.61–1.59 (m, 4H, 2 × CH_2), 1.51–1.45 (m, 6H, 3 × CH_2). ^{13}C NMR (100 MHz, DMSO-d_6) $\delta =$ 182.6 (C, C-4), 164.6 (C, C-7′), 163.4 (C, C-2), 163.2 (C, pyr–CO), 160.8 (C, C-6), 158.2 (C, C-5), 154.6 (C, C-9), 154.0 (CH, pyr–C2), 153.0 (C, C-4′), 151.9 (C, C-7), 139.0 (C, C-4″), 138.7 (CH, pyr–C4), 130.5 (2 × CH, C-2″, C-6″), 129.8 (2 × CH, C-2′, C-6′), 129.0 (2 × CH, C-3″, C-5″), 128.6 (2 × CH, C-3′, C-5′), 127.8 (C, pyr–C3), 123.3 (C, C-10), 123.1 (CH, pyr–C5), 112.0 (CH, C-3), 106.1 (CH, C-8), 62.7 (CH_2, CH_2N), 54.4 (2 × CH_2, 2 × CH_2N), 45.8 (2 × CH_2, 2 × CH_2N), 25.9 (2 × CH_2, 2 × CH_2CH_2N), 24.7 (2 × CH_2, 2 × ***C***H_2CH_2N), 24.3 (2 × CH_2, 2 × CH_2***C***H_2CH_2). ESI-MS (*m/z*): 676.2 [M+H]$^+$. HRESIMS *m/z* (pos): 676.2620 $C_{39}H_{38}N_3O_8$ (calcd. 676.2653).

*2-(4-((4-((4-benzylpiperazin-1-yl)methyl)benzoyl)oxy) phenyl)-5,6-dihydroxy-4-oxo-4H-chromen-7-yl 6-(piperidin-1-yl)nicotinate (**7d**)*

Yellow solid, yield: 62.2 %, m.p. 273–275 °C.1H-NMR (400 MHz, DMSO-d_6): $\delta = 12.94$ (brs, 1H, 5-OH), 8.75 (s, 1H, pyr–H_2), 8.18 (d, $J = 8.8$ Hz, 2H, Ar″–$H_{2,6}$), 8.08 (d, $J = 8.0$ Hz, 2H, Ar′–$H_{2,6}$), 8.01 (dd, $J_1 = 9.2$ Hz, $J_2 = 2.4$ Hz, 1H, pyr–H_4), 7.50–7.46 (m, 4H, Ar″–$H_{3,5}$ and Ar′–$H_{3,5}$), 7.29–7.18 (m, 5H, Ar–H), 7.02 (s, 1H, Ar–H_8), 6.89 (d, 1H,

$J = 9.2$ Hz, pyr–H_5), 6.68 (s, 1H, Ar–H_3), 3.68–3.66 (m, 4H, 2 × CH_2N), 3.55 (s, 2H, CH_2N), 3.44 (s, 2H, CH_2N), 2.37 (m, 8H, 4 × CH_2), 1.62–1.52 (2m, 6H, 3 × CH_2). ^{13}C NMR (100 MHz, DMSO-d_6) $\delta = 182.7$ (C, C-4), 164.7 (C, C-7′), 163.4 (C, C-2), 163.3 (C, pyr–CO), 160.8 (C, C-6), 157.9 (C, C-5), 154.6 (C, C-9), 154.0 (CH, pyr–C2), 153.1 (C, C-4′), 152.0 (C, C-7), 139.1 (C, C-4″), 138.5 (CH, pyr–C4), 130.5 (2 × CH, C-2″, C-6″), 129.7 (2 × CH, C-2′, C-6′), 129.4 (2 × CH, Ph–C), 128.9 (2 × CH, C-3″, C-5″), 128.7 (2 × CH, C-3′, C-5′), 128.7 (2 × CH, Ph–C), 127.8 (C, pyr–C3), 127.5 (CH, Ph–C), 123.3 (C, C-10), 123.0 (CH, pyr–C5), 112.0 (CH, C-3), 106.1 (CH, C-8), 62.5 (CH_2, CH_2N), 62.1 (CH_2, $PhCH_2N$), 53.2 (2 × CH_2, 2 × CH_2N), 53.0 (2×CH_2, 2×CH_2N), 45.9 (2×CH_2, 2×CH_2N), 25.7 (2×CH_2, 2×***C***H_2CH_2N), 24.8 (CH_2, CH_2***C***H_2CH_2). ESI-MS (*m/z*) 767.3 $[M+H]^+$. HRESIMS *m/z* (pos): 767.3038 $C_{45}H_{43}N_4O_8$ (calcd. 767.3075).

*5,6-dihydroxy-2-(4-((4-(morpholinomethyl)benzoyl)oxy) phenyl)-4-oxo-4H-chromen-7-yl 6-(piperidin-1-yl) nicotinate (**7e**)*

Yellow solid, yield: 39.6 %, m.p. 247–249 °C. ^{1}H-NMR (400 MHz, DMSO-d_6): δ 13.00 (brs, 1H, 5-OH), 8.94 (s, 1H, pyr–H_2), 8.24 (d, $J = 8.4$ Hz, 2H, Ar″–$H_{2,6}$), 8.15–8.07 (m, 3H, Ar′–$H_{2,6}$, pyr–H_4), 7.59–7.52 (m, 4H, Ar′-$H_{3,5}$, Ar″-$H_{3,5}$), 7.08 (s, 1H, Ar–H_8), 7.01–6.95 (m, 1H, pyr–H_5), 6.75 (s, 1H, Ar–H_3), 3.70–3.61 (m, 10H, 2 × CH_2N, 2 × CH_2O, ArCH_2N), 2.51–2.49 (m, 4H, 2 × CH_2N), 1.54–1.52 (m, 6H, 3 × CH_2). ^{13}C NMR (100 MHz, DMSO-d_6) $\delta =$ 182.8 (C, C-4), 164.5 (C, C-7′), 163.9 (C, C-2), 163.2 (C, pyr–CO), 160.6 (C, C-6), 158.1 (C, C-5), 154.8 (C, C-9), 154.1 (CH, pyr–C2), 153.4 (C, C-4′), 151.8 (C, C-7), 138.9 (C, C-4″), 138.5 (CH, pyr–C4), 130.8 (2 × CH, C-2″, C-6″), 129.5 (2 × CH, C-2′, C-6′), 128.7 (2 × CH, C-3′, C-5′), 128.2 (2 × CH, C-3″, C-5″), 127.8 (C, pyr–C3), 123.4 (C, C-10), 123.1 (CH, pyr–C5), 112.3 (CH, C-3), 103.9 (CH, C-8), 72.7 (2 × CH_2, 2 × CH_2O), 63.1 (CH_2, CH_2N), 54.5 (2 × CH_2, 2 × CH_2N), 45.7 (2 × CH_2, 2 × CH_2N), 24.9 (2 × CH_2, 2 × ***C***H_2CH_2N), 24.2 (CH_2, CH_2***C***H_2CH_2). ESI-MS (*m/z*): 678.2 $[M+H]^+$. HRESIMS *m/z* (pos): 678.2420 $C_{38}H_{36}N_3O_9$ (calcd. 678.2446).

*5,6-dihydroxy-2-(4-((4-(morpholinomethyl)benzoyl)oxy) phenyl)-4-oxo-4H-chromen-7-yl 6-morpholinonicotinate (**7f**)*

Yellow solid, yield: 43.1 %, m.p. 253–255 °C.^{1}H-NMR (400 MHz, DMSO-d_6): $\delta = 12.94$(s, 1H, 5-OH), 8.74 (s, 1H, pyr–H2), 8.20 (d, $J = 12.0$Hz, 2H, Ar″–$H_{2,6}$), 8.13 (d, $J =$ 8.0Hz, 2H, Ar′–$H_{2,6}$), 8.02 (dd, $J_1 = 9.2$ Hz, $J_2 = 2.4$ Hz, 1H, pyr–H_4), 7.64 (m, 2H, Ar″–$H_{3,5}$), 7.50 (d, $J = 8.8$Hz, 2H, Ar′–$H_{3,5}$), 7.03 (s, 1H, Ar–H_8), 6.90 (d, 1H, $J = 9.6$ Hz, pyr–H_5), 6.78 (s, 1H, Ar–H_3), 3.69–3.66 (m, 8H, 4 × CH_2O), 3.33–3.25 (m, 6H, 3 × CH_2N), 2.47–2.45 (m, 4H, 2 × CH_2N). ^{13}C NMR (100 MHz, DMSO-d_6) $\delta = 182.7$ (C, C-4), 164.6 (C, C-7′), 163.4 (C, C-2), 163.1 (C, pyr–CO), 160.8 (C, C-6), 157.7 (C, C-5), 154.1 (C, C-9), 153.4 (CH, pyr–C2), 152.6 (C, C-4′), 151.4 (C, C-7), 138.5 (C, C-4″), 138.2 (CH, pyr–C4), 130.1 (2 × CH, C-2″, C-6″), 128.4 (2 × CH, C-2′, C-6′), 128.1 (2 × CH, C-3″, C-5″), 122.8 (2 × CH, C-3′, C-5′), 122.4 (C, pyr–C3), 111.4 (C, C-10), 105.6 (CH, pyr–C5), 104.9 (CH, C-3), 103.9 (CH, C-8), 72.5 (2 × CH_2, 2 × CH_2O), 72.3 (2 × CH_2, 2 × CH_2O), 63.1 (CH_2, CH_2N), 45.3 (4 × CH_2, 4 × CH_2N). ESI-MS (*m/z*): 680.5 $[M+H]^+$. HRESIMS *m/z* (pos): 680.2243 $C_{37}H_{34}N_3O_{10}$ (calcd. 680.2239).

*Evaluation of physiochemical properties of compounds **7a–f***

In vitro stability testing was carried out as previously described (Cao et al., 2006). Briefly, the test compound (1 mg) was dissolved in DMSO (20 µL) to provide a stock solution, which was then diluted with distilled water to a concentration of 0.2 mg/mL. Aliquots (200 µL) of the diluted solution were added to phosphate-buffered saline (2 mL, pH = 2.0 or 7.4), and maintained at 37 ± 0.5 °C in screw-capped vials in a water bath. The samples were withdrawn at appropriate time intervals, and analyzed by HPLC. For solubility testing, distilled water (50 µL) was added to the test compound (3–5 mg). The mixture was ultrasonicated and filtered through a microporous membrane filter (0.45 µm). The saturated solution was then serially diluted with distilled water and the solubility of the compound was calculated using standard curves. HPLC analyses were performed using a high performance liquid chromatography instrument (LC-10AVP, Shimadzu, Japan). Separation was carried out on an Agilent C18 column (4.6 mm × 150 mm, 5 µm), with gradient elution (methanol/0.1 % H_3PO_4; 0–50 min, 40–60 %). The column temperature was maintained at 40 °C and the flow rate was 1.0 mL/min. The results were summarized in Table 1.

Caco-2 cell permeability assay

Caco-2 cell culture

Caco-2 cells were seeded onto Millicell^{TM} Caco-2 plates at a density of 1.0×10^5 cells/cm^2. The cells were cultured in Dulbecco's modified Eagle's medium (DMEM) supplemented with 10 % fetal bovine serum and containing penicillin (100 U/mL), streptomycin (100 U/mL), $NaHCO_3$ (3.7 g/L) and L-glutamine (1 %). The cells were grown at 37 °C in a humidified incubator with an atmosphere of 5 % CO_2.

Table 1 The physiochemical properties for target compounds (**7a–f**) and reference compounds

Compounds	Solubility [a]	Stability in PBS ($t_{1/2}$ h)	
	(μg/mL)	pH = 2.0	pH = 7.4
Scutellarin	65.9	—	—
Scutellarein	14.4	—	5.5
7a	183.64	>72	8.3
7b	176.45	>72	7.4
7c	60.22	>72	4.2
7d	324.43	>72	8.7
7e	291.89	>72	5.2
7f	224.16	>72	5.4

[a] The solubility for target compounds were tested in pH = 2.0 phosphate buffer

*Caco-2 cell-based permeability assay of compounds **7a–f***

Caco-2 cells were seeded at a density of 1×10^5 cells/cm^2 on a six-well Millicell^{TM} plate and allowed to grow for 21 days to reach confluence and differentiate. The integrity and transportation ability of the Caco-2 cell monolayer were examined by measuring the transepithelial electrical resistance (TEER) using an epithelial voltohmmeter (Millicell-ERS electrical resistance system, Millipore, Bedford, MA, USA). Inserts with TEER values > 300 Ω cm^2 in the culture medium were selected for transport experiments. On day 21, the Caco-2 cell monolayer was washed three times with pre-warmed (37 °C) serum-free DMEM and equilibrated using the same medium. To determine the rate of drug transport in the apical to basolateral direction, solutions of the test compound (200 μM, 0.2 mL), scutellarin (200 μM, 0.2 mL) and scutellarein (200 μM, 0.2 mL) were added to the apical plate (AP). The transport basolateral plate (BL) was filled with pre-warmed (37 °C) serum-free DMEM (1.2 mL). To determine the transport rate in the basolateral to apical direction, solutions of the test compound (200 μM, 1.2 mL), scutellarin (200 μM, 1.2 mL) and scutellarein (200 μM, 1.2 mL) were added to the BL and the filter wells (apical plate, AP) were filled with pre-warmed (37 °C) serum-free DMEM (0.2 mL). For analysis of the test compound, scutellarin and scutellarein, aliquots (200 μL) of the DMEM solutions were taken from the AP or BL side, methanol (50 μL) was added and the mixtures were centrifuged at 13000 g for 10 min. Aliquots (10 μL) of the supernatant solutions were analyzed by UPLC-MS/MS, using established methods, as described below.

UPLC-MS/MS conditions for analysis of test compounds

Ultra performance liquid chromatography (UPLC) analyses were performed using a Waters ACQUITY UPLC instrument. The samples were separated on a BEH C l8 column (2.1 mm × 50 mm, 1.7 μm), equipped with a Waters BEH C18 VanGuard pre-column (2.1 mm × 5 mm, 1.7 μm). The mobile phase consisted of acetonitrile containing 0.1 % formic acid (A) and water containing 0.1 % formic acid (B). The elution gradient was as follows: 10–90 % A (0–3 min) and 10 % A (3–4 min). The mobile phase flow rate was 0.35 mL/min, the column temperature was 45 °C and the injection volume for the permeability assay was 5 μL. Mass spectrometry identifications were carried out using a Waters ACQUITY TQD (triple quadrupole mass spectrometer), equipped with a Z-spray ESI source and connected to an ACQUITY UPLC system. The acquisition parameters were as follows: collision gas, argon; nebulizing, and drying gas, nitrogen; source temperature, 120 °C; desolvation temperature, 350 °C; cone gas flow rate, 50 L/h; desolvation gas flow rate, 650 L/h; collision gas flow rate, 0.16 mL/min; and capillary voltage, 3.0 kV. Selected ion monitoring mode was used; in positive ion mode (ESI^+), the confirmation ions (*m/z*) were: 463.1 (scutellarin), 286.9 (scutellarein), 662.3 (**7a**), 662.3 (**7b**), 678.3 (**7c**), 767.0 (**7d**), 678.3 (**7e**), and 680.5 (**7f**). Cone voltages were 40, 45, 50, 40, 40, 45, 40, and 45 V, respectively. All of the assays were carried out in triplicate in at least three separate experiments. Results are expressed as mean ± SEM and statistical significance was analyzed by one-way analysis of variance (ANOVA) followed by Dunnett's multiple comparison test using Origin scientific statistics software, version 8.0. The results are summarized in Table 2 and Fig.1.

In vitro BBB permeability assay

Primary culture of rat brain microvessel endothelial cells (BMECs) and astrocytes

Brains were removed from five 2-weeks old Sprague-Dawley rats, the hemispheres were washed, the cerebella removed, and the meninges peeled off. The white matter was removed and the gray matter was collected and stored in cold DMEM before use. The gray matter was washed three times with D-Hank solution, digested successively for 40 min with 0.1 % type II collagenase containing 0.005 % DNase I and 0.1 % collagenase/dispase, and then centrifuged at 800 g for 5 min at 4 °C. The pellets were resuspended in DMEM and filtered through nylon mesh (150 μm). The filtrate was collected, centrifuged at 800 g for 5 min at 4 °C and 20 % mass fraction of bovine serum albumin was then added to suspend the sediment. The resulting suspension was centrifuged at 1000 g for 20 min at 4 °C. The sediment was washed with DMEM and centrifuged at 800 g for 5 min at 4 °C. The resulting sediment was resuspended in 44 % mass fraction of Percoll and centrifuged at 1000 g for 10 min at 4 °C to provide high purity brain

Table 2 Apparent permeability coefficients (P_{app}) of target compounds (**7a–f**) and reference compounds in Caco-2 cells

compounds	$P_{app\ AP\ to\ BL} \times 10^{-6}$(cm/s)[a]	$P_{app\ BL\ to\ AP} \times 10^{-6}$(cm/s)[a]	ER($P_{app\ BL\ to\ AP}/P_{app\ AP\ to\ BL}$)[b]
Scutellarin(I)[d]	0.53 ± 0.11[c]	1.05 ± 0.21	1.98
Scutellarein(II)	0.83 ± 0.21	1.46 ± 0.24	1.76
7a	1.42 ± 0.33	2.30 ± 0.47	1.62
7b	3.11 ± 0.87	2.94 ± 0.38	0.94
7c	1.93 ± 0.54	2.91 ± 0.67	1.51
7d	0.70 ± 0.13	1.26 ± 0.22	1.80
7e	1.97 ± 0.38	1.91 ± 0.35	0.97
7f	1.67 ± 0.42	1.69 ± 0.44	1.01

[a] $P_{app\ A\ to\ B}$: transport of the compound from apical to basolateral; $P_{app\ B\ to\ A}$: transport of the compound from basolateral to apical. [b] ER ($P_{app\ B\ to\ A}/P_{app\ A\ to\ B}$): the ratio of $P_{app\ B\ to\ A}$ to $P_{app\ A\ to\ B}$. [c] Data were mean ± SD ($n = 3$). [d] The concentration of test compounds was at 200 μM for scutellarin, scutellarein and compounds **7a–f**. The incubation time was up to 120 min

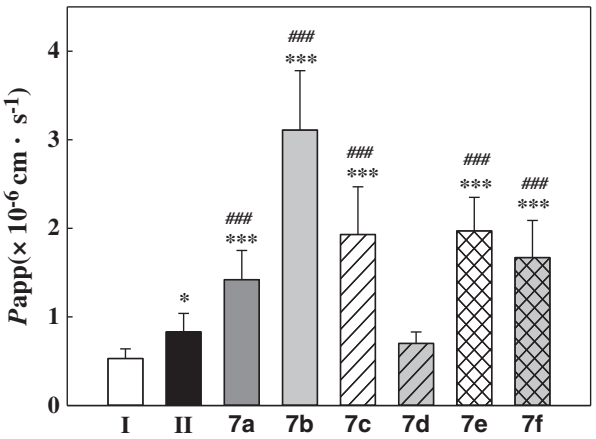

Fig. 1 The apical to basolateral apparent permeability coefficients ($P_{app\ AP\ to\ BL}$) of 4′-N-substituted (aminomethyl) benzoate-7-substituted nicotinic acid ester derivatives (**7a–f**), scutellarin and scutellarein in Caco-2 cells (mean ± SD, $n = 3$). $^{***}P < 0.001$ as compared with scutellarin(I) group. $^{###}P < 0.001$ as compared with scutellarein (II) groups

microvascular section. The brain microvascular section was then seeded in a culture bottle for primary culture. The resulting rat BMECs were resuspended in EGM-2 endothelium cell growth medium containing 5 % fetal bovine serum, seeded into a rat tail collagen-coated flask containing puromycin (4 mg/mL) and grown to confluence. Primary cultures of rat BMECs were identified using an inverted microscope and by rabbit anti-factor VIII fluorescence immunocytochemistry. Astrocyte primary cultures were prepared as previously described (Biegel et al., 1995) and identified using rabbit anti-glial fibrillary acidic protein (GFAP) in fluorescence immunocytochemistry.

Establishment of an in vitro BBB model comprising a co-culture of BMECs, astrocytes and brain microvascular perithelial cells (BMPCs)

The in vitro BBB model using primary BMECs, astrocytes and BMPCs was established on rat tail collagen/fibronectin (7.5 μg/mL)-coated 24-well polycarbonate Transwell filter inserts (12 mm membrane diameter, 1.12 cm^2 growth surface area, 0.4 μm pore size) (Corning Costar Quality Biological, Gaithersburg, MD, USA). The astrocytes and BMPCs were seeded onto one side of the filter at a density of 1.5×10^4 cells per insert and allowed to adhere to the side of the filter for 6 h. After 3 days the rat BMECs were seeded onto the other side of the filter at a density of 2.0×10^4 cells per filter and the Transwell plate was cultured in EGM-2 medium at 37 °C under an atmosphere containing 5 % CO_2. In vitro experiments using the BBB cell model were conducted within 3–4 days of seeding the rat BMECs. TEER was measured using a Millicell-ERS electrical resistance system. Only cell layers with TEER values > 300 Ω/cm^2 were used for the transport assays. Permeability of sodium fluorescein, expression of alkaline phosphatase and γ-glutamyl transpeptidase, and scanning electron microscopy were used to confirm the integrity of the in vitro BBB model.

In vitro BBB permeability assay

Transport experiments were performed by simultaneously adding final concentrations (25, 100, 400 μM) of test compounds (**7a–c**, **7e** and **7f**), dissolved in serum-free DMEM, to the apical side (AP, 0.2 mL) and serum-free DMEM to the basolateral side (BL, 1.2 mL). For determination of time-dependent transport of test compounds, aliquots (60 μL) were taken from the BL medium after 20, 40, 60, 80, 100, 120, 140, 160, and 180 min and immediately replaced by an equivalent volume of serum-free DMEM. Aliquots (60 μL) were collected from the BL side after 90 min to determine the $P_{app\ AP\ to\ BL}$ values of the test compounds. Results obtained using UPLC-MS/MS detection were consistent with those obtained in the Caco-2 cell-based permeability assay. All of the assays were carried out in triplicate in at least three separate experiments. Results are expressed as mean ± SEM and statistical significance was analyzed by ANOVA followed by Dunnetts's multiple comparison test using Origin scientific statistics software, version 8.0. The results are summarized in Table 3, Fig. 2a and 2b.

Results and discussion

4′-*N*-substituted (aminomethyl) benzoate-7-substituted nicotinic acid ester derivatives of scutellarein (**7a–f**) were

Table 3 Apparent permeability coefficients and efflux rate of target compounds (**7a–f**) and reference compounds in BBB cell layer

Compound	$P_{app\ AP\ to\ BL} \times 10^{-6}(cm{\cdot}s^{-1})$[a]	$P_{app\ BL\ to\ AP} \times 10^{-6}(cm{\cdot}s^{-1})$[a]	ER($P_{app\ BL\ to\ AP}/P_{app\ AP\ to\ BL}$)[b]
Scutellarin(I)[d]	0.17 ± 0.08[c]	0.37 ± 0.13	2.18
Scutellarein(II)	0.18 ± 0.06	0.34 ± 0.09	1.89
7a	0.59 ± 0.11	1.12 ± 0.20	1.89
7b	1.65 ± 0.37	1.06 ± 0.15	0.64
7c	0.56 ± 0.12	0.50 ± 0.18	0.90
7e	1.01 ± 0.13	0.96 ± 0.11	0.95
7f	0.71 ± 0.16	1.35 ± 0.27	1.90

[a] $P_{app\ A\ to\ B}$: transport of the compound from apical to basolateral; $P_{app\ B\ to\ A}$: transport of the compound from basolateral to apical. [b] ER ($P_{app\ B\ to\ A}/P_{app\ A\ to\ B}$): the ratio of $P_{app\ B\ to\ A}$ to $P_{app\ A\ to\ B}$. [c] Data were mean ± SD ($n = 3$). [d] The concentration of test compounds was at 200 μM for scutellarin, scutellarein and compounds **7a–f**. The incubation time was up to 120 min

obtained using straightforward synthetic methods. Evaluation of physiochemical properties (Table 1) showed that compounds **7a–f** are more stable ($t_{1/2} > 72$ h) under acidic conditions (pH = 2) than under neutral conditions (pH = 7.4, $t_{1/2}$ 4.2–8.7 h). Except for compound **7c**, the solubilities of the test compounds (**7a–f**) (176.45–324.43 μg/mL) were significantly higher than those of scutellarein (14.4 μg/mL) or scutellarin (65.9 μg/mL). The solubilities of compounds **7d**, **7e**, and **7f** (324.43 μg/mL, 291.89 μg/mL and 224.16 μg/mL, respectively) are 22.5-fold, 20.2-fold, and 15.6-fold higher than that of scutellarein.

In the Caco-2 cell permeability assay (Table 2), compound **7d** had an efflux ratio (ER, $P_{app\ BL\ to\ AP}/P_{app\ AP\ to\ BL}$) of 1.80, which is higher than the ER (1.76) of scutellarein. The ERs of the other test compounds were in the range 0.94–1.62 and were thus lower than those of scutellarin and scutellarein. The ER values of **7a**, **7c**, **7d**, and **7f** were >1.0, whereas the ER values of **7b** and **7e** were <1.0, indicating greater permeability in the BL to AP direction for compounds **7a**, **7c**, **7d**, and **7f** than for compounds **7b** or **7e**. The Caco-2 cell permeabilities of **7b**, **7c**, and **7e** ($P_{app\ AP\ to\ BL}$ values of $3.11 \pm 0.87 \times 10^{-6}$ cm/s, $1.93 \pm 0.54 \times 10^{-6}$ cm/s and $1.97 \pm 0.38 \times 10^{-6}$ cm/s, respectively) were 5.9-fold, 3.6-fold, and 3.7-fold higher than that of scutellarin ($0.53 \pm 0.01 \times 10^{-6}$ cm/s) and 3.7-fold, 2.3-fold, and 2.4-fold higher than that of scutellarein ($0.83 \pm 0.21 \times 10^{-6}$ cm/s). Compound **7b** had the highest $P_{app\ AP\ to\ BL}$ value ($3.11 \pm 0.87 \times 10^{-6}$ cm/s) and the lowest ER value (0.94) (Fig.1). Compounds **7b**, **7d**, and **7e** have significantly higher Caco-2 cell permeability than scutellarin or scutellarein, indicating that 4′-*N*-substituted (aminomethyl) benzoic acid esterification and 7-nicotinic acid esterification of scutellarein would significantly enhance gut absorptive capacity.

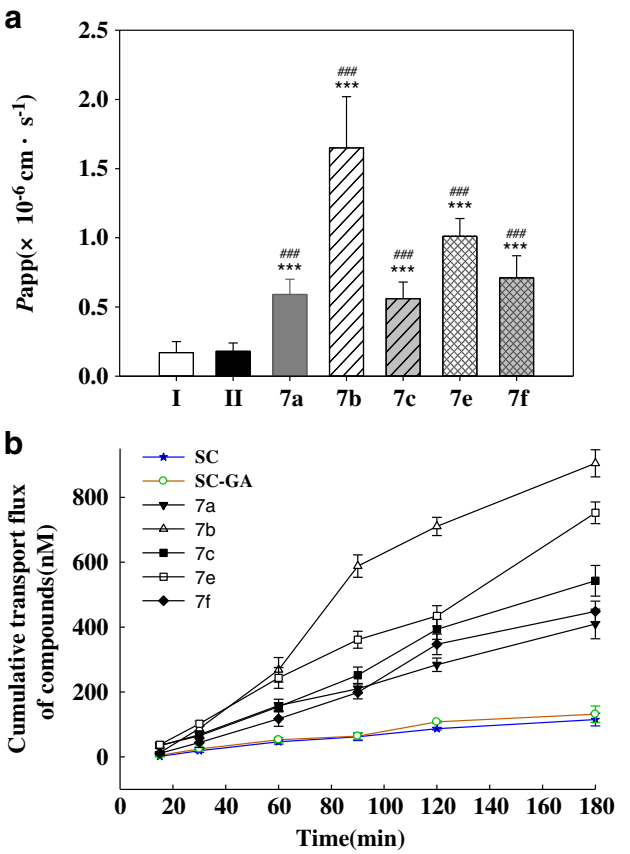

Fig. 2 **a** Apparent permeability coefficients of compounds from apical to basolatearl in BBB cell layer. The data were represented as mean ± SE ($n = 3$). $^{***}P < 0.001$ vs. scutellarin(I); $^{\#\#\#}P < 0.001$ vs. scutellarein (II). **b** Apical to basolatearl cumulative transport flux of target compounds (**7a–f**), scutellarin(I) and scutellarein(II) (200 μM) across the BBB cell layer at different time intervals

The $P_{app\ AP\ to\ BL}$ values across the BBB cell layer for compounds (**7a–c**, **7e** and **7f**) are summarized in Table 3. Permeabilities of all test compounds ($P_{app\ AP\ to\ BL}$ values $0.56 \pm 0.12 \times 10^{-6}$ cm/s to $1.65 \pm 0.37 \times 10^{-6}$ cm/s) were significantly higher than those of scutellarin ($0.17 \pm 0.08 \times 10^{-6}$ cm/s) or scutellarein ($0.18 \pm 0.08 \times 10^{-6}$ cm/s). The in vitro BBB permeability of **7b**, **7e**, and **7f** ($P_{app\ AP\ to\ BL}$ values $1.65 \pm 0.37 \times 10^{-6}$ cm/s, $1.01 \pm 0.13 \times 10^{-6}$ cm/s and $0.71 \pm 0.16 \times 10^{-6}$ cm/s, respectively) were 9.7-fold, 5.9-fold, and 4.2-fold higher than that of scutellarin ($0.17 \pm 0.08 \times 10^{-6}$ cm/s) and 9.2-fold, 5.6-fold, and 3.9-fold higher than that of scutellarein ($0.18 \pm 0.06 \times 10^{-6}$ cm/s). Compound **7b** had the highest $P_{app\ AP\ to\ BL}$ value ($1.65 \pm 0.37 \times 10^{-6}$ cm/s) and the lowest ER value (0.64) (Fig. 2a). Permeability of the test compounds **7a–f** across the BBB cell layer increased linearly with time (0–180 min) and the permeabilities of compounds **7a–f** were significantly higher than those of scutellarin or scutellarein at all time points (Fig. 2b). The obtained results confirm our hypothesis that introduction of a nicotinic acid ester moiety at the 7-position

of 4′-*N*-substituted (aminomethyl) benzoate derivatives of scutellarein should increase BBB permeability compared with the parent drug. We propose that this increased permeability can be attributed to transport by the MCT1 expressed on the luminal and abluminal membranes of brain capillary endothelial cells (Tachikawa et al., 2011).

Acknowledgments This work was supported by the grants from National Natural Science Foundation of China (NSFC Nos. 81260473, 81460523), Projects of Guizhou Science and Technology Department (Nos. 2013-3031, 2012-3013), and Excellent Youth Scientific Talents Foundation of Guizhou Province (No. 2013-45).

Compliance with ethical standards

Conflict of interest The authors declare that they have no competing interests.

References

Bartzatt R (2005) Applying pattern recognition methods and structure property correlations to determine drug carrier potential of nicotinic acid and analogize to dihydropyridine. Eur J Pharm Biopharm 59:63–71

Biegel D, Spencer DD, Pachter JS (1995) Isolation and culture of human brain microvessel endothelial cells for the study of blood-brain barrier properties *in vitro*. Brain Res 692:183–189

Bonina FP, Arenare L, Ippolito R, Boatto G, Battaglia G, Bruno V, de Caprariis P (2000) Synthesis, pharmacokinetics and anticonvulsant activity of 7-chlorokynurenic acid prodrugs. Int J Pharm 202:79–88

Bradbury MW (1984) The structure and function of the blood-brain barrier. Fed Proc 43:186–190

Cao F, Guo JX, Ping QN, Liao ZG (2006) Prodrugs of scutellarin: ethyl, benzyl and N,N-diethylglycolamide ester synthesis, physiochemical properties, intestinal metabolism and oral bioavailability in the rats. Eur J Pharm Sci 29:385–393

Che QM, Pan LY, Chen Y, He H (2007) Study on pharmacokinetics of scutellarein in Rats. Chin Pharmacol J 42:1418–1421

Chen XY, Cui L, Duan XT, Ma B, Zhong DF (2006) Pharmacokinetics and metabolism of the flavonoid scutellarin in humans after a single oral administration. Drug Metab Disp 34:1345–1352

Chen ZW, Hu YZ, Wu HH, Jiang HD (2005) Synthesis and vasorelaxation action of flavonoids. Acta Pharm Sin 40:1001–1007

Dai ZQ, Su H, Luo M, Ou Y, Fu XZ, Dong YX, Cha YF, Zhang S, Huang Y, Wang YL (2015) Application of N-substituted (aminomethyl)benzoate Strategy in Design of Scutellarein Derivatives with Improved Caco-2 Cell Permeability and In Vitro Antioxidative Activity. B Korean Chem Soc doi: 10.1002/bkcs.10377

Enerson BE, Drewes LR (2003) Molecular features, regulation, and function of monocarboxylate transporters: implications for drug delivery. J Pharm Sci 92:1531–1544

Fu XZ, Xing FJ, Lan YY, Wang AM, Wang YL, Li J, Zhou W, Zhang W, Liu Y (2011) Synthesis and in vitro anti-oxidative activity studies of 4'-N-substituted- aminomethyl-benzoate derivatives of scutellarein. Chinese J Org Chem 31:1043–1048

Fu XZ, Zhang W, Wang YL, Lan YY, Wang AM, Zhou W, Huang Y, Li J, Xing FJ, Liu Y (2011) Design, synthesis and anti-oxidative evaluation of L-amino acid prodrugs of scutellarein. Acta Pharm Sin 46:548–555

Ge QH, Zhou Z, Zhi XJ, Ma LL, Chen XH (2003) Pharmacokinetics and absolute bioavailability of breviscapine in beagle dogs. Chin J Pharm 34:618–620

Hansch C, Björkroth JP, Leo A (1987) Hydrophobicity and central nervous system agents: on the principle of minimal hydrophobicity in drug design. J Pharm Sci 76:663–687

Hong H, Liu GQ (2000) Protection against hydrogen peroxide-induced cytotoxicity in PC12 cells by scutellarin. Life Sci 74:2959–2973

Hu XM, Zhou MM, Hu XM, Zeng FD (2005) Neuroprotective effects of scutellarin on rat neuronal damage induced by cerebral ischemia/reperfusion. Acta Pharmacol Sin 26:1454–1459

Ju WZ, Zhang J, Tan HS, Jiang M, Chen W, Xiong NN (2005) Determination of scutellarin in human plasma by LC-MS method and its clinical pharmacokinetics in Chinese healthy volunteers. Chin J Clin Pharmcol Ther 10:298–301

Malakoutikhah M, Teixidó M, Giralt E (2008) Toward an optimal blood-brain barrier shuttle by synthesis and evaluation of peptide libraries. J Med Chem 51:4881–4889

Pan Z, Feng T, Shan L, Cai B, Chu W, Niu H, Lu Y, Yang B (2008) Scutellarin-induced endothelium-independent relaxation in rat aorta. Phytother Res 22:1428–1433

Rajesh K (2014) Synthesis, alkylating activity and physiochemical study of nitrogen mustard agent for brain delivery. Int J Phar Teach Pract 5:925–929

Sang ZP, Qiang XM, Li Y, Wu B, Zhang H, Zhao MG, Deng Y (2015) Design, synthesis, and biological evaluation of scutellarein carbamate derivatives as potential multifunctional agents for the treatment of Alzheimer's disease. Chem Biol Drug Des doi: 10.1111/cbdd.12580

Sang Z, Qiang X, Li Y, Yuan W, Liu Q, Shi Y, Ang W, Luo Y, Tan Z, Deng Y (2015) Design, synthesis and evaluation of scutellarein-O-alkylamines as multifunctional agents for the treatment of Alzheimer's disease. Eur J Med Chem 94:348–366

Tachikawa M, Murakami K, Martin PM, Hosoya K, Ganapathy V (2011) Retinal transfer of nicotinate by H^+-monocarboxylate transporter at the inner blood-retinal barrier. Microvasc Res 82:385–390

Wang Y, Ao H, Qian Z, Zheng Y (2011) Intestinal transport of scutellarein and scutellarin and first-pass metabolism by UDP-glucuronosyltransferase-mediated glucuronidation of scutellarein and hydrolysis of scutellarin. Xenobiotica 41:538–548

Wu ZY, Pan J, Yuan Y, Hui AL, Yang Y, Zhou A, Tao M, Zhou XJ (2012) Brain-targeting research of 10-O-nicotinate ginkgolide B: a new prodrug of ginkgolide B. Med Chem Res 21: 4028–4036

Young RC, Mitchell RC, Brown TH, Ganellin CR, Griffiths R, Jones M, Rana KK, Saunders D, Smith IR, Sore NE (1988) Development of a new physiochemical model for brain penetration and its application to the design of centrally acting H2 receptor histamine antagonists. J Med Chem 31:656–671

Zhang JL, Che QM, Li SZ, Zhou TH (2003) Study on metabolism of scutellarin in rats by HPLC-MS and HPLC-NMR. J Asian Nat Prod Res 5:249–256

Zhang WD, Chen WS, Wang YH, Yang GJ, Kong DY, Li HT (2000) Studies on the flavone glycosides from the extract of. Erigeron breviscapus. Chin Tradit Herb Drugs 31:565–568

Zhang ZR, Luo WZ, Nagai T (2011) Hydrolyslis kinetics and photolysis kinetics of N_1-retinoyl-5-flurouracil. STP Pharma Sci 11:243–246

Zhou QS, Jiang XH, Yu JR, Li KJ (2006) Synthesis and characterization of PEG-scutellarin conjugates, a potential PEG ester prodrug for the oral delivery of scutellarin. Chin Chem Lett 17:85–88